



ELSEVIER

Available online at [www.sciencedirect.com](http://www.sciencedirect.com)

SCIENCE @ DIRECT®

Vacuum 76 (2004) 389–392

VACUUM  
SURFACE ENGINEERING, SURFACE INSTRUMENTATION  
& VACUUM TECHNOLOGY

[www.elsevier.com/locate/vacuum](http://www.elsevier.com/locate/vacuum)

# Diagnostics of Trivelpiece-Gould mode produced discharges

N. Djermanova, O. Ezekiev, Zh. Kiss'ovski, St. Kolev, A. Shivarova\*

*Faculty of Physics, Sofia University, 5 J. Bourchier Blvd., BG-1164 Sofia, Bulgaria*

## Abstract

The paper presents results on the spatial structure of 27-MHz discharges sustained in a diffusion-controlled regime by the wave field of Trivelpiece-Gould modes. Methods of probe diagnostics of high-frequency discharges with magnetized plasma production are applied.

© 2004 Elsevier Ltd. All rights reserved.

*Keywords:* High-frequency discharges; Probe diagnostics; Magnetized plasma production; Trivelpiece-Gould modes

## 1. Introduction

The involvement in the plasma processing technology [1] of discharges with magnetized plasma production in the field of Trivelpiece-Gould (TG) modes provokes interest in detailed studies of the space distribution of their parameters. The latter requires methods of local measurements and motivates diagnostics of the discharges by electrical probes. The obtained results [2,3] giving indications for comparatively high-density plasmas at low gas pressure (moreover, produced with high efficiency [3–5]) stimulate further investigations of the discharge properties.

A recent study [3] by probe diagnostics of the radial structure of 27-MHz diffusion-controlled argon discharges produced by TG-modes is

extended here towards results on the axial variations of plasma density  $n$  and electron temperature  $T_e$ . The data processing is based on a numerical procedure developed for applying the theory [6,7] of a thick sheath around a cylindrical probe. The discussions are based on the influence of gas pressure and magnetic field strength on the axial discharge structure.

## 2. Experimental arrangements and data-processing procedure

The experimental set-up (Fig. 1) is the same as used before [3]. Argon discharges produced in an external magnetic field are sustained in a glass tube (with radius of  $R = 2.4$  cm and length of  $L = 1.5$  m) by TG-modes at a frequency  $f = 27$  MHz. A double-ring coupler is the wave launcher. The ranges of variation of the

\*Corresponding author. Fax: +359-2-962-5276

E-mail address: [ashiva@phys.uni-sofia.bg](mailto:ashiva@phys.uni-sofia.bg) (A. Shivarova).

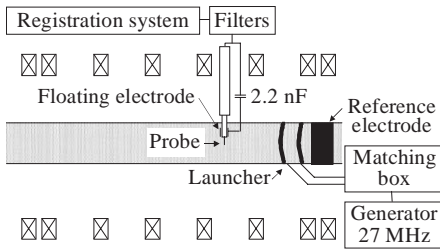


Fig. 1. Experimental set-up.

gas-pressure and the magnetic field are, respectively,  $p = 1.3\text{--}27\text{ Pa}$  and  $B_0 = 0.04\text{--}0.1\text{ T}$ .

A radially movable single Langmuir probe is used (Fig. 1). A passive compensation [3] of the high-frequency field is applied in order to avoid the distortions of the probe characteristics.

It is well-known [8,9] that, for given gas discharge conditions, the travelling-wave-sustained discharges (TWSDs) extend in length with the increase of the applied power  $P_0$  while the values of the plasma density at the discharge end and of the axial gradient  $dn/dz$  of the plasma density remain the same. Thus, the axial profiles of the plasma parameters can be measured by varying the applied power and using a probe fixed at a given  $z$ -position.

Methods of probe diagnostics of unmagnetized plasmas can be applied to magnetized plasmas provided the inequalities  $r_p < r_{Le}$  and  $r_p \ll r_{Li}$  (where  $r_{Le,i}$  are the electron- and ion gyro-radii) are fulfilled. According to this, a thin probe (with a radius of  $r_p = 0.05\text{ mm}$ ) is used in the experiment. Since  $r_p < \lambda_D$  (where  $\lambda_D$  is the Debye length), the ABR-theory [6,7] for thick sheaths around the probe is applied for processing of the probe characteristics: Fig. 2 shows numerical results for the ion saturation current  $I_i$  of current–voltage characteristics obtained for a cylindrical probe. The normalized quantities are:  $\eta_p = -eV_p/\kappa T_e$  (with  $e$  and  $\kappa$  being, respectively, the electron charge and the Boltzmann constant, and  $V_p$  the probe voltage),  $\xi_p = r_p/\lambda_D$  and  $J = I_i(2\pi\kappa T_e l)^{-1} \sqrt{m_i/2\varepsilon_0 n}$ , where  $l$  is the length of the probe ( $l = 4\text{ mm}$ ),  $m_i$  is the ion mass and  $\varepsilon_0$  is the vacuum permittivity. The plasma density is obtained from a comparison of the measured ion saturation current with the numerical results.

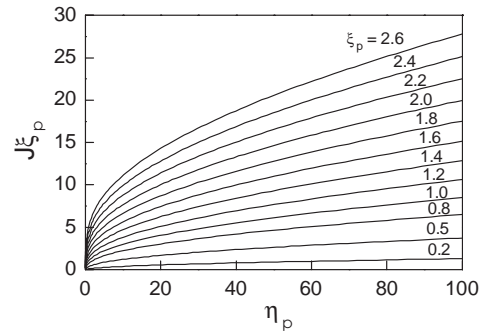


Fig. 2. Theoretical results (in normalized quantities) for the ion saturation-current parts of probe characteristics.

### 3. Results and discussion

Figs. 3–5 present the experimental results for axial profiles of the plasma density  $n(z)$  for three values of the external magnetic field. Changes of  $n(z)$  with gas-pressure variations are shown. According to the experimental arrangements (Fig. 1), the results are for the main part of the discharge excluding its end and the region close to the wave launcher.

Due to the comparatively low value of the wave frequency ( $\omega = 2\pi f = 1.7 \times 10^8\text{ s}^{-1}$ ), the discharge is maintained under conditions of strong collisions in the total gas-pressure range studied: the ratio ( $v_{e-a}/\omega$ ), where  $v_{e-a}$  is the elastic electron-neutral collisions frequency, is high ( $v_{e-a}/\omega = 0.45\text{--}2.5$ ). Thus, the space damping rate  $\alpha$  of the wave strongly increases with  $(\omega/\omega_p)$ , where  $\omega_p$  is the plasma frequency, and the wave produces high-density plasmas [3,9,10]. Owing to this, the 27-MHz discharges appear as sources of comparatively dense plasmas even at low gas pressure.

In the whole range of the  $B_0$ -variation in the experiment, the TG-modes propagate in strongly magnetized plasmas:  $\Omega_e \gg \omega \gg \Omega_i$ , where  $\Omega_{e,i}$  are the electron- and ion-gyrofrequencies. In accordance with the theoretical results [11,12] on discharge maintenance by TG-modes, the experimental results (Figs. 3–5) show a linear decrease of the plasma density over the main part of the discharge measured. The magnetic field strongly influences the ambipolar diffusion losses: the second term in the denominator of the transverse

ambipolar-diffusion coefficient  $D_{A\perp} = D_{Az}/[1 + (m_i \Omega_i \Omega_e / \mu_{i-a} v_{i-a} v_{e-a})]$  is very large, especially for the lowest gas pressure. (Here,  $D_{Az}$  is the axial ambipolar-diffusion coefficient,  $\mu_{i-a}$  is the reduced

mass for elastic ion–neutral collisions and  $v_{i-a}$  is their frequency.) This results in positively charged walls and an electron wall sheath, as confirmed by the more negative values of the plasma potential measured (not shown here) at the discharge axis, compared to the pre-sheath region.

Since  $v_{i-a}$  is the factor determining the space damping rate  $\alpha$  in high-density plasmas, moreover, with strong collisions [10,13], and  $\alpha$  controls the behaviour of the axial gradient  $dn/dz$  of the plasma density in TWSDs [9,10,12],  $dn/dz$  appears to be proportional to  $p$  (Figs. 3–5).

At low gas pressure,  $dn/dz$  decreases with the magnetic field increase (from  $4 \times 10^7$  to  $3 \times 10^7 \text{ cm}^{-4}$ ). In this case  $D_{A\perp} \ll D_{Az}$ , and according to the model [11] of discharges in a strong  $B_0$  ( $\Omega_e \gg \omega, \omega_p, v_{e-a}$ ), the wave-plasma self-consistency [9–12] expressed by the relation between  $n$  and the wave-field intensity  $|E|^2 \approx |E_z|^2$  [11], is ensured by axial diffusion. The decrease of the wave-field intensity along the discharge length predicted by the model [11] is confirmed by the slight decrease of the electron temperature (Fig. 4).

The comparison of the experimental results (Fig. 6) for the radial profiles of the plasma density obtained at different axial positions with Bessel-type of profiles [ $n(r, z) = n(r = 0, z) \times J_0(\mu r/R)$ ] shows slight decrease of the parameter  $\mu$  of the radial plasma-density inhomogeneity towards the discharge end.

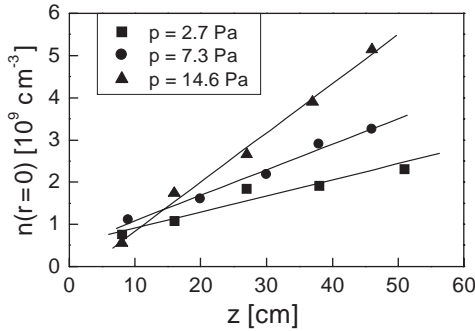


Fig. 3. Axial profiles of the plasma density at different gas pressures and  $B_0 = 0.046 \text{ T}$ . Experimental results (symbols) approximated by linear dependences (solid lines).  $z = 0$  is the position of the discharge end.

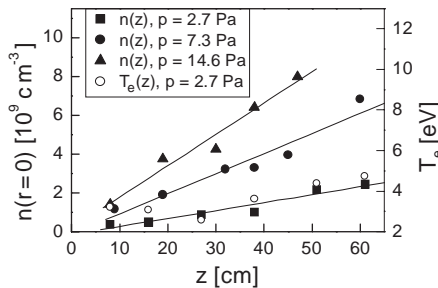


Fig. 4. The same as in Fig. 2, but for  $B_0 = 0.062 \text{ T}$ . In addition, experimental data for the axial profile of the electron temperature at  $p = 2.7 \text{ Pa}$  are presented.

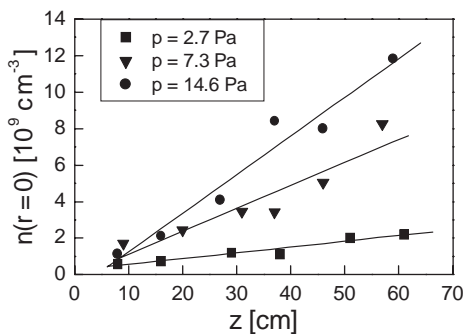


Fig. 5. The same as in Fig. 2, but for  $B_0 = 0.095 \text{ T}$ .

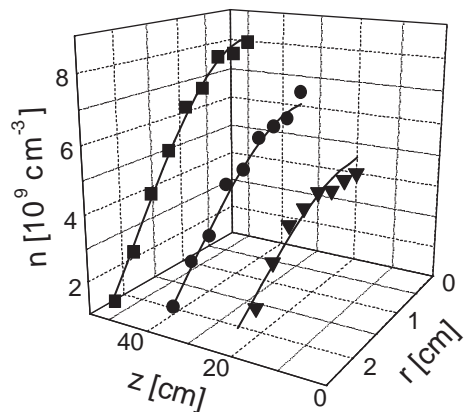


Fig. 6. Radial profiles of the plasma density ( $p = 14.6 \text{ Pa}$ ,  $B_0 = 0.062 \text{ T}$ ): experimental results (symbols) compared with Bessel-function profiles (curves).

#### 4. Conclusions

The study provides experimental results on the structure of low-pressure high-frequency gas discharges sustained in the wave field of TG-modes. The influence of changing gas pressure and magnetic field strength on the discharge behaviour, in the case of strong plasma magnetization, is shown.

#### Acknowledgements

This work is part of the Shared Cost EURATOM project FU05-CT-2002-00092 and Project no 1007 of the National Science Fund in Bulgaria.

#### References

- [1] Margot J, Chaker M, Moisan M, St-Onge L, Bounasri F, Dallaire A, Gat E. In: Williams PF, editor. *Plasma processing in semiconductors*. Dordrecht: Kluwer; 1997. p. 491.
- [2] Margot J, Vidal F, Chaker M, Johnston TW, Aliouchouche A, Tabbal M, Delprat S, Pauna O, Benhabib D. *Plasma Sources Sci Technol* 2001;10:556–66.
- [3] Djermanova N, Kiss'ovski Zh, Kolev St, Schlüter H, Shivarova A, Tarnev Kh. *Vacuum* 2003;69:147–52.
- [4] Pasquiers S, Boisse-Laporte C, Granier A, Bloyet E, Leprince P, Marec J. *J Appl Phys* 1989;65:1371–6.
- [5] Kiss'ovski Zh, Shivarova A, Tarnev Kh. In: Pisarczyk P, et al., editors. *Proceedings of the 24th ICPIG*. vol. 1. Warsaw: Space Research Center, Polish Academy of Sciences;1999. p. 209.
- [6] Allen JE, Boyd RLF, Reynolds P. *Proc Phys Soc London, Sec B* 1957;70:297–305.
- [7] Annaratone BM, Allen MW, Allen JE. *J Phys D* 1992;25:417–24.
- [8] Moisan M, Ferreira CM, Hajlaoui Y, Henry D, Hubert J, Pantel R, Ricard A, Zakrzewski Z. *Rev Phys Appl* 1982;17:707–27.
- [9] Aliev Yu M, Schlüter H, Shivarova A. *Guided-wave-produced plasmas*. Berlin: Springer; 2000.
- [10] Makasheva K, Shivarova A. *Phys Plasmas* 2001;8: 836–45.
- [11] Shivarova A, Tarnev Kh. *J Phys D* 1998;31:2543–9.
- [12] Schlüter H, Shivarova A, Tarnev Kh. *Contrib Plasma Phys* 2003;43:206–15.
- [13] Schlüter H, Shivarova A, Tarnev Kh. *J Electromagn Waves Appl* 2002;16:37–58.